



# *Candida albicans* ENT2 Contributes to Efficient Endocytosis, Cell Wall Integrity, Filamentation, and Virulence

Christiane Rollenhagen,<sup>a,b</sup> Harrison Agyeman,<sup>a</sup> Susan Eszterhas,<sup>a,b</sup>  Samuel A. Lee<sup>a,b</sup>

<sup>a</sup>Medicine Service, White River Junction VA Medical Center, White River Junction, Vermont, USA

<sup>b</sup>Geisel School of Medicine at Dartmouth, Hanover, New Hampshire, USA

**ABSTRACT** Epsins play a pivotal role in the formation of endocytic vesicles and potentially provide a linkage between endocytic and other trafficking pathways. We identified a *Candida albicans* epsin, *ENT2*, that bears homology to the *Saccharomyces cerevisiae* early endocytosis genes *ENT1* and *ENT2* and studied its functions by a reverse genetic approach utilizing CRISPR-Cas9-mediated gene deletion. The *C. albicans ent2Δ/Δ* null mutant displayed cell wall defects and altered antifungal drug sensitivity. To define the role of *C. albicans ENT2* in endocytosis, we performed assays with the lipophilic dye FM4-64 that revealed greatly reduced uptake in the *ent2Δ/Δ* mutant. Next, we showed that the *C. albicans ent2Δ/Δ* mutant was unable to form hyphae and biofilms. Assays for virulence properties in an *in vitro* keratinocyte infection model demonstrated reduced damage of mammalian adhesion zippers and host cell death from the *ent2Δ/Δ* mutant. We conclude that *C. albicans ENT2* has a role in efficient endocytosis, a process that is required for maintaining cell wall integrity, hyphal formation, and virulence-defining traits.

**IMPORTANCE** The opportunistic fungal pathogen *Candida albicans* is an important cause of invasive infections in hospitalized patients and a source of considerable morbidity and mortality. Despite its clinical importance, we still need to improve our ability to diagnose and treat this common pathogen. In order to support these advancements, a greater understanding of the biology of *C. albicans* is needed. In these studies, we are focused on the fundamental biological process of endocytosis, of which little is directly known in *C. albicans*. In addition to studying the function of a key gene in this process, we are examining the role of endocytosis in the virulence-related processes of filamentation, biofilm formation, and tissue invasion. These studies will provide greater insight into the role of endocytosis in causing invasive fungal infections.

**KEYWORDS** *Candida albicans*, biofilm, endocytosis, filamentation, pathogenesis, secretion, membrane trafficking

In prior work, we demonstrated that prevacuolar and late-stage secretion are required for secretion of Saps and lipases and the virulence-related processes of filamentation and biofilm formation (1, 2). We also demonstrated that prevacuolar secretion is required for virulence utilizing both *in vitro* and *in vivo* models of infection (3). Interestingly, many of these anterograde secretory pathways also appear to contribute to retrograde or endocytic pathways. However, the role of endocytic trafficking in *Candida albicans* filamentation, biofilm formation, and virulence remains understudied, despite its importance as a fundamental component of the secretory pathway (4, 5).

Endocytosis has been studied in detail in the model yeast *Saccharomyces cerevisiae* (6) and begins at the plasma membrane as a highly coordinated and complex process. It ultimately delivers endocytic membranes and cargo to the yeast vacuole while intersecting with exocytic and other secretory pathways. The best understood endocytic pathway

**Citation** Rollenhagen C, Agyeman H, Eszterhas S, Lee SA. 2021. *Candida albicans ENT2* contributes to efficient endocytosis, cell wall integrity, filamentation, and virulence. mSphere 6:e00707-21. <https://doi.org/10.1128/mSphere.00707-21>.

**Editor** Aaron P. Mitchell, University of Georgia  
This is a work of the U.S. Government and is not subject to copyright protection in the United States. Foreign copyrights may apply.  
Address correspondence to Samuel A. Lee, [samuel.a.lee@dartmouth.edu](mailto:samuel.a.lee@dartmouth.edu).

**Received** 18 August 2021

**Accepted** 19 September 2021

**Published** 29 September 2021

in *S. cerevisiae* occurs via clathrin-mediated endocytosis, a temporally orchestrated process involving many proteins that interact in a highly coordinated manner (7–17).

Early endocytosis in *S. cerevisiae* is mediated by the early coat proteins clathrin, AP-2p, Ede1p, Syp1p, and Pal1p (9). Subsequently, the endocytic vesicle matures with the recruitment of middle and late coat proteins, including Sla2p, followed by the epsins Ent1p and Ent2p, which interact with the GTPase Cdc42p (10, 11). The key late coat proteins Pan1p and End3p bind to Sla2p, Ent1p, and Ent2p, which couples these proteins to the actin endocytic machinery, followed by membrane invagination and endocytosis (12–14).

Epsins are accessory proteins and serve as adaptor molecules that provide a bridge for cargo selectivity and vesicle formation to facilitate endocytosis (18, 19). Their two main functions are the induction of membrane bending, which is needed for invagination, and the binding and loading of cargo into vesicles (18, 19). In *S. cerevisiae*, *ENT1* and *ENT2* encode epsin-like proteins that function as key mediators of endocytosis (10). *ENT1* and its paralog *ENT2* arose from the whole-genome duplication event in *S. cerevisiae*. Both genes have an epsin N-terminal homology (ENTH) domain at the N-terminal domain and clathrin-binding domain at the C terminus (10). Ent1p and Ent2p are negatively regulated by Prk1p-mediated phosphorylation (20). Interestingly, whereas Ent1p and Ent2p share similar functions, there is evidence that they have additional divergent functions and cellular localization (20, 21). Deletion of both *ENT1* and *ENT2* together is synthetically lethal in *S. cerevisiae*. This phenotype can be rescued by reintroducing an ENTH domain (10).

The ENTH domain plays a critical role in binding GTPase-activating proteins (GAPs) involved in regulation of Cdc42p, which is a key mediator of cell polarity (22). Recent studies have shown that this domain binds the phosphorylated head group of the lipid phosphatidylinositol-4,5-bisphosphate (PIP<sub>2</sub>), disturbing the plasma membrane bilayer's stability, thereby contributing to membrane curvature (23, 24). Ent1p and Ent2p facilitate membrane curvature as the ENTH domain regulates membrane dynamics (25, 26). The epsins Ent1p and Ent2p might have a later role in vesicle formation by binding to Ede1p (also known as Eps15p), a protein found at the rim of budding coated vesicles (27). Another interesting feature of Ent1p and Ent2p is a ubiquitin-interacting motif (UIM) (27) that interacts with cargo. The plasma membrane PIP<sub>2</sub> is also required for efficient recruitment of these cargo molecules (24). UIM has been demonstrated to internalize the Ena1p pump. It requires phosphorylation of an upstream Ser/Thr-rich motif and ubiquitylation in the cytoplasmic domain, which binds UIMs of Ent1p and Ent2p, and Ede1p (28). As a consequence of these interactions, Ena1p is endocytosed and transported toward degradative vacuolar/lysosomal compartments or recycling routes (28).

In a recently published screen for novel inhibitors of filamentation in *C. albicans*, several compounds were identified that inhibit fluid-phase endocytosis (29), thus suggesting a biological intersection between filamentation and endocytosis that could be exploited as antifungal therapy (29, 30). Our studies demonstrate roles for *ENT2* in efficient endocytosis that have subsequent effect on cell wall integrity, filamentation, and virulence.

## RESULTS

**Identification of *C. albicans ENT2* as the ortholog of *S. cerevisiae ENT1/2*.** A BLASTp search of the *Candida* Genome Database retrieved only one ortholog of *S. cerevisiae* Ent1p. This ortholog was identified as C2\_01390W, alias *C. albicans ENT2*, which consists of a 1,569-bp intronless open reading frame (*orf19.1444*), predicted to encode a 522-amino-acid product. A BLASTp search of *S. cerevisiae* Ent2p homology retrieved the same *Candida* Ent2p protein and identified very weak homologies to *C. albicans* Ent3p and to a portion of Ent4p.

Figure 1 shows a protein alignment analysis of five homologous epsin-like products of *S. cerevisiae* (*ENT1* and *ENT2*), and *C. albicans ENT2*, *ENT3*, and *ENT4*. The comparison

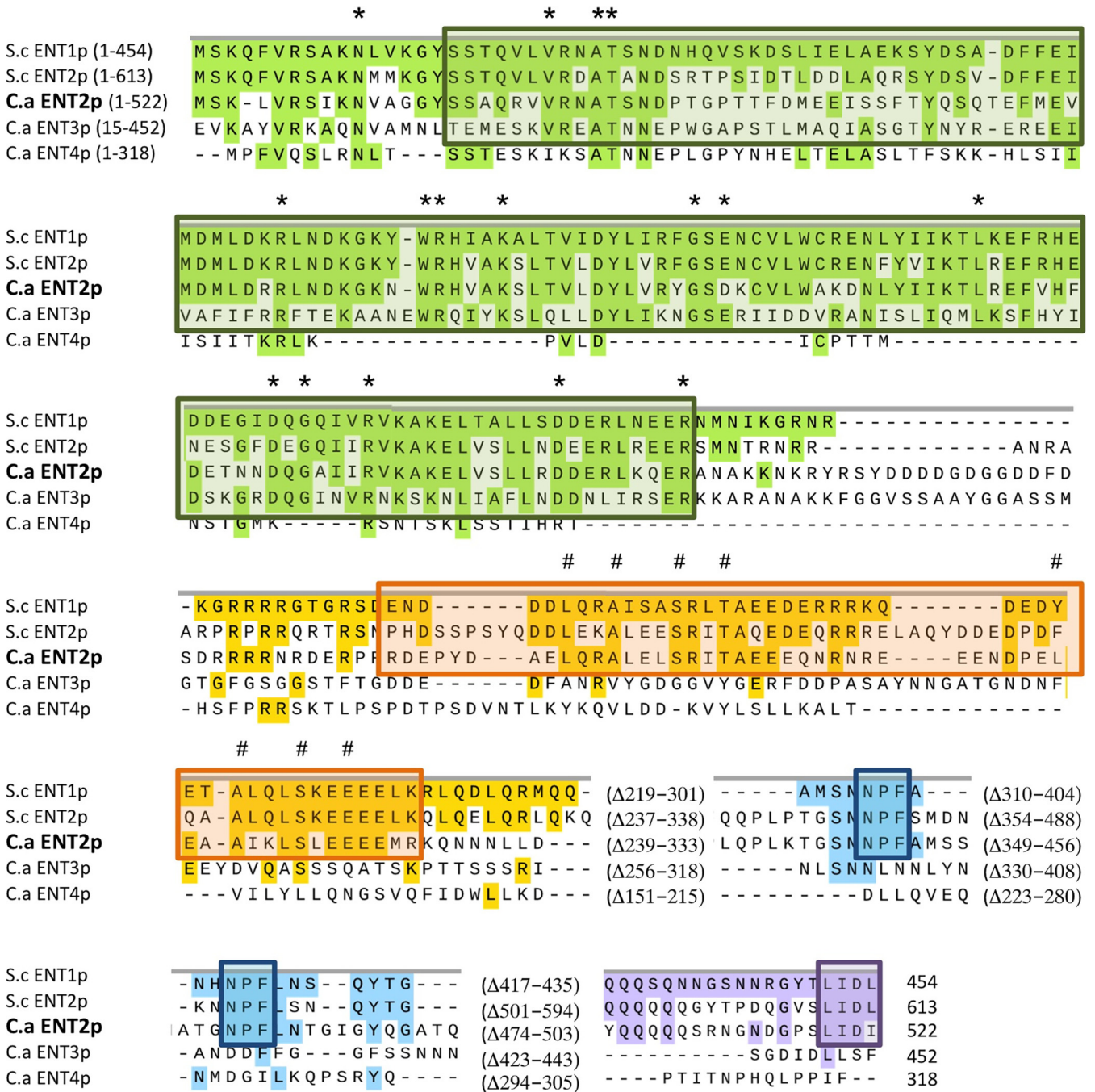


**FIG 1** *C. albicans* Ent2p bears a strong homology to *S. cerevisiae* Ent1p/Ent2p. Shown is the alignment of *S. cerevisiae* (S.c) Ent1p and Ent2p with *C. albicans* (C.a) Ent2p, Ent3p, and Ent4p. Amino acids conserved to greater than 60% are shaded. The green boxes identify the ENTH domain. The highly conserved sequences of the ENTH domain are marked with an asterisk. The orange block delimits the pair of UIM motifs with # symbols marking the locations of conserved amino acids. Regions of low complexity and conservation have been omitted, and the extent of the omission is indicated (Δ amino acid numbers). Blue boxes indicate the tripeptide, NPF, and the purple block is the yeast clathrin-binding motif. Note that *C. albicans* Ent3p is presented starting from amino acid 15.

between paralogous *S. cerevisiae* Ent1p and Ent2p indicates an overall 56% identity and 68% similarity of amino acid sequences. The local homology is particularly striking in the ENTH domain, a region identified as an epsin-like N-terminal homology (31). The *C. albicans* Ent2p ortholog likewise shows a strong resemblance to *S. cerevisiae* Ent1p (43% identity, 56% similarity) particularly in the ENTH domain, where 61% of the amino acids are identical and 78% are similar. *C. albicans* Ent3p has much weaker homology (23% identity, 37% similarity) and is most pronounced only in the ENTH domain region.

Ent4p homology is even weaker than Ent3p homology. Of particular note are the residues marked by asterisks that were found to be highly conserved in the ENTH domains from disparate organisms (31); these are well conserved in all but Ent4p. The conservation of the amino acid sequence of *C. albicans* Ent2p in pathogenic fungi is largely confined to the ENTH domain with the striking exception of the hypothetical protein CTRG\_01231p in *Candida tropicalis* strain MYA-3404; CTRG\_01231p shares 80% amino acid identity (86% similarity) with *C. albicans* Ent2p (see Fig. S2 in the supplemental material).

In addition to the ENTH domains, there are features involved in endosomal trafficking which are conserved between *S. cerevisiae* Ent1/2 proteins and *C. albicans* Ent2p but absent in *C. albicans* Ent3p and Ent4p. A pair of ubiquitin-interacting motifs (UIMs) adjacent to the ENTH domain is seen in *C. albicans* Ent2p as well as in the *S. cerevisiae* paralogs Ent1p and Ent2p. UIMs are responsible for the recognition of ubiquitin and cargo binding, a function important for cargo specificity in endocytosis and other endosomal trafficking (32–35). In contrast, *C. albicans* Ent3p and Ent4p lack these motifs, making it unlikely to function as a paralog for *C. albicans* Ent2p. The tripeptide arginine-proline-phenylalanine (NPF) is involved in interactions among endocytic proteins (36); it is found in two places in *C. albicans* Ent2p and *S. cerevisiae* Ent1p and Ent2p but again is not present in Ent3p and Ent4p. Much of the remainder of *C. albicans* Ent2p is low complexity with little conservation aside from a preponderance of glutamines (Q). In *S. cerevisiae* Ent2p, the Q-rich region is believed to form coiled coils that contribute to protein-protein binding (37). The Q-rich stretches are also a feature largely absent in *C. albicans* Ent3p and Ent4p. Finally, at the C-terminal end of the proteins, *C. albicans* Ent2p and *S. cerevisiae* Ent1p and Ent2p have clathrin-binding sequences that conform to the variant consensus identified in yeast by Wendland (10) and Dell'Angelica (38). There are no identifiable clathrin-binding sequences in *C. albicans* Ent3p and Ent4p.

On the basis of these analyses of the predicted protein structure of *C. albicans* Ent2p, we propose it is the best candidate for a functional ortholog to *S. cerevisiae* Ent1/2p. Compared to *C. albicans* Ent2p, Ent3p and Ent4p are lacking several functional domains and have only weak homology in their ENTH domain, making similar functions unlikely.

**Construction of a *C. albicans ent2Δ/Δ* mutant.** We then sought to determine the function of *C. albicans ENT2* using a reverse genetic approach. We used a PCR-based CRISPR-Cas9 method to generate a *C. albicans ent2Δ/Δ* null mutant (knockout [KO]) and corresponding complemented, or “knock-in” (KI) strain, where both copies of the wild-type allele were reintroduced into the *ent2Δ/Δ* null mutant. Correct strain construction was confirmed by Southern blotting. The probe labeled a 5,276-bp BstXI-digested fragment for the wild type (wt) and KI as well as a smaller 3,720-bp fragment lacking the *ENT2* for the KO. This result is shown in Fig. S1, confirming the expected genotype of the *ent2Δ/Δ* null mutant strain.

**Contribution of *ENT2* to growth, viability, and cell morphology.** To address whether the *ent2Δ/Δ* null mutant (KO) has a growth defect, we grew the KO strain and the control strains, the wild type and knock-in strains, at 30°C in liquid YNB (yeast nitrogen base) medium with glucose or on YPD (yeast extract-peptone-dextrose) agar. The KO had a modestly reduced growth of about 25% average over time compared to the wt and KI in liquid media (Fig. 2A). We observed an initial growth delay in the KO that was carried throughout the recorded time at 2.5 to 5 h of culture growth compared to the wt and KI control strains. The doubling time was moderately increased by 0.33 h during this time from 2.21 h for wt and KI to 2.54 h for the KO. On YPD plates, this modest growth defect in the KO was also evident (Fig. 2B). We did not detect temperature sensitivity when growing the strains at 37°C (Fig. 2C). While the cell size and morphology of the KO appeared to be like those of the wt and KI strains (Fig. 2D, DIC), staining with calcofluor white (CW) revealed an increased fluorescent signal associated with the cell wall in this KO strain compared to wt and KI controls (Fig. 2D and E). This finding motivated us to further investigate cell wall integrity and function.

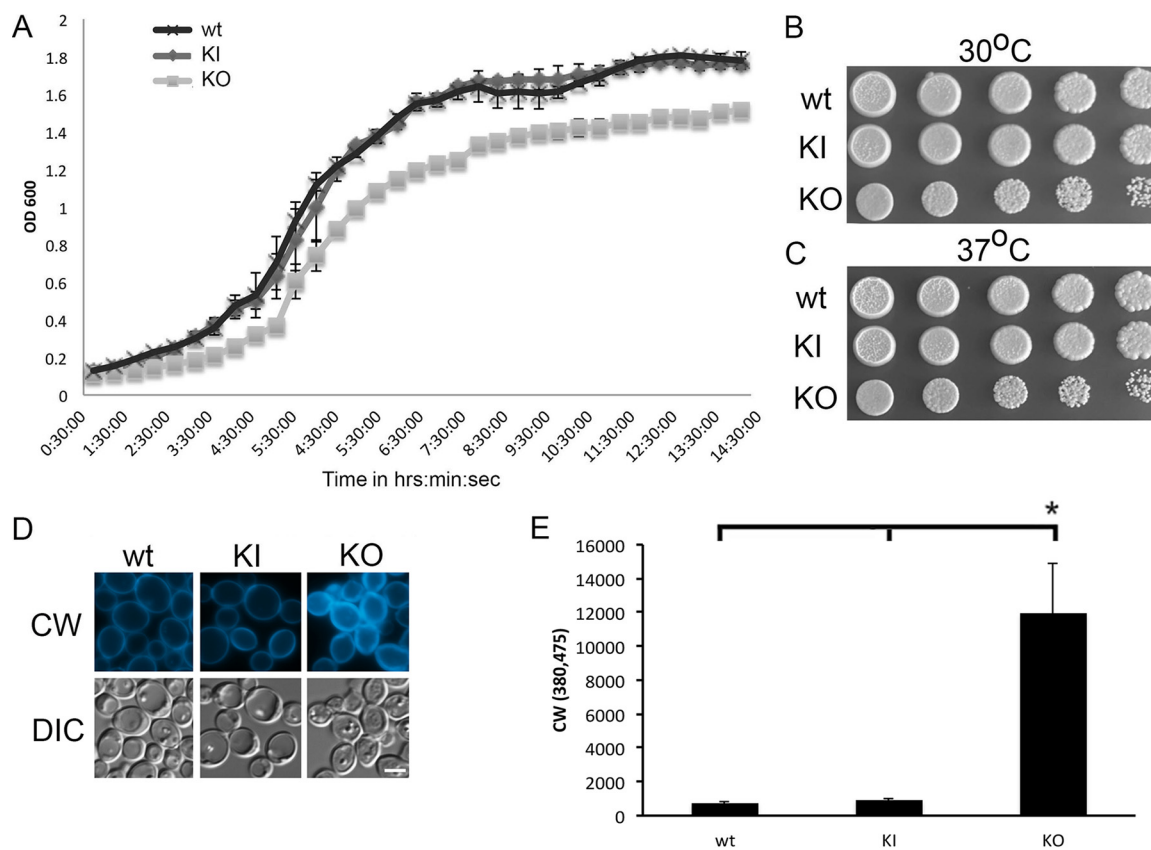


**FIG 2** The *ent2Δ* null mutant strain has a modest growth defect. (A to E) The *ent2Δ/Δ* null mutant strain (knockout [KO]), wild type (wt), and knock-in strain (KI) were depicted in a growth curve (A), on YPD plates incubated for 48 h at 30°C (B) or 37°C (C), visualized by DIC and fluorescence microscopy stained with calcofluor white (CW) (D), as well as in a CW quantification assay (E). The bar in panel D is 5  $\mu$ m. The images shown in panels B to D are representative of three different experiments. Error bars in panels A and E are the standard deviations of three different data sets. Each individual data point was run in triplicate and averaged. Statistical significance between control strains (wt and KI) and the KO strain was determined with Student's *t* test (\*,  $P < 0.05$ ).

**The *C. albicans ent2Δ/Δ* strain has a defect in endocytosis.** In order to define the role of *ENT2* in *C. albicans* endocytosis and intracellular membrane trafficking, we used the lipophilic fluorescent dye FM4-64 as described previously (39). FM4-64 is inserted into the outer plasma membrane and endocytosed via clathrin-based endocytosis in an energy-dependent manner, where it binds the inner membranes, including the vacuolar membrane.

The results of this experiment demonstrated that the *ent2Δ/Δ* mutant strain (KO) did not accumulate FM4-64 in the vacuolar membrane compared to control strains (Fig. 3A and B). The images in Fig. 3A revealed that the staining of FM4-64 in the KO strain is heterogenous, with some cells exhibiting increased signal intensity. This finding was comparable to the result when *ent2Δ/Δ* cells were incubated on ice, a condition that inhibits endocytosis (Fig. S5). To exclude the possibility of toxicity, we performed a lactate dehydrogenase (LDH) assay to confirm whether viability of the KO is similar to the viability of control strains and found no significant difference (Fig. S3). Next, the signal of FM4-64 labeling the vacuolar membrane increased over time in the wt and the KI and is consistent with normal endocytosis (Fig. 3B). These findings strongly suggest that *C. albicans* Ent2p is a critical component needed to enable efficient clathrin-based endocytosis.

**Contribution of *ENT2* to cell wall stressors and salt stress tolerance.** To assess the role of *ENT2* in response to cell wall stress, we assayed the *ent2Δ/Δ* mutant (KO), wild-type, and knock-in strains on YPD plates containing sodium dodecyl sulfate (SDS) (0.05%), calcofluor white (50  $\mu$ g/ml), or Congo red (140  $\mu$ g/ml) at 30°C. Under these three growth conditions, the KO had a dramatic growth defect compared to wt and KI

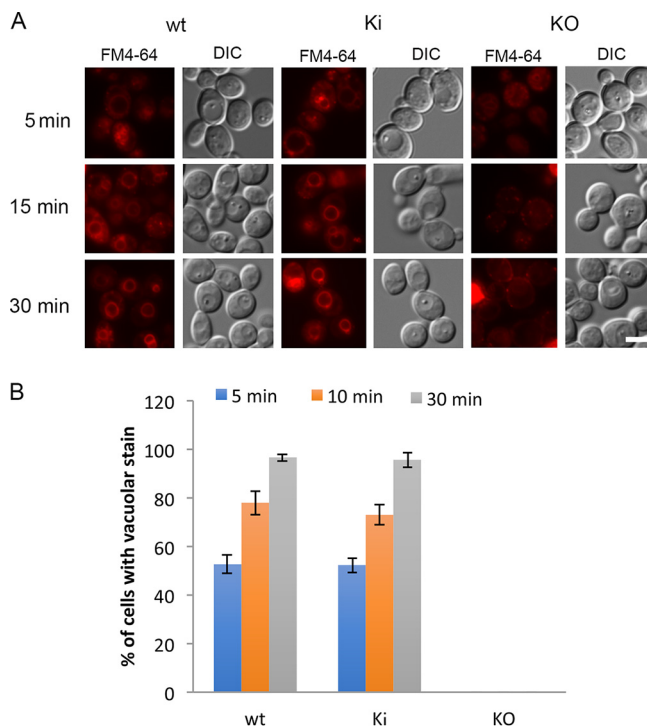


**FIG 3** The *ent2Δ/Δ* mutant strain has delayed endocytosis and accumulates dye in the vacuole. (A) Fluorescent images of *ent2Δ/Δ* null mutant (KO) and control strains, wild type (wt), and knock-in (KI) strains stained with the lipophilic fluorescent dye FM4-64 are shown after incubation of 5, 15, and 30 min at room temperature (RT). (B) Quantitative analysis of the vacuolar stain in wt, KI, and KO strains after an incubation of 5, 15, and 30 min at RT. The images shown in panel A are representative of three different experiments. The bar in panel A is 5  $\mu$ m. Error bars in panel B are the standard deviations from three different data sets expressed as percentage of the total number of cells.

when grown at 30°C (Fig. 4A), in contrast to the modest growth defect on YPD agar. We further tested whether the KO's cell wall defects impacted adhesion to plastic surfaces (polystyrene) in RPMI 1640 medium. The adhesion capacity of the KO was increased by approximately 30% compared to control strains (wt and KI) after 2 h of incubation. Interestingly, when cells grew for 24 h on plastic surfaces, the KO strain kept a constant adhesion capacity over time, while the control strains increased their adhesion levels (Fig. 4B). These findings are likely linked to a change in cell morphology in the control strains but not in the KO, as the growth conditions (RPMI 1640 medium) and plastic surfaces induce filamentous growth.

We then addressed whether the *ent2Δ/Δ* null mutant is sensitive to salt stress. The *S. cerevisiae* homolog *ENT1/2* is known to facilitate endocytosis of Ena1p, a primary plasma membrane Na<sup>+</sup>-ATPase exporter (40–43) that transports Na<sup>+</sup>, K<sup>+</sup>, and Li<sup>+</sup> ions (44–47). Thus, we challenged the KO strain with 500 mM KCl, NaCl, or 100 mM LiCl in an agar plate assay. LiCl prevented KO growth, while the control strains were not affected. The KO demonstrated a mild growth defect on NaCl compared to wt and KI, while on KCl, there was no growth defect compared to the YPD control plate (Fig. 4C). These findings suggest that *C. albicans ENT2* contributes to efficient Li<sup>+</sup> and Na<sup>+</sup> ion export.

***C. albicans ent2Δ/Δ* sensitivity to antifungal agents.** To test whether the defects in cell wall structure, cation transport, and adhesion correlated with altered sensitivity to antifungal agents, we tested three commonly used antifungal drugs, fluconazole, caspofungin, and amphotericin B. Fluconazole is a fluorine-substituted, bis-triazole antifungal agent. It functions by interrupting the conversion of lanosterol to ergosterol by binding to fungal cytochrome P-450 leading to the disruption of fungal membranes. Its function

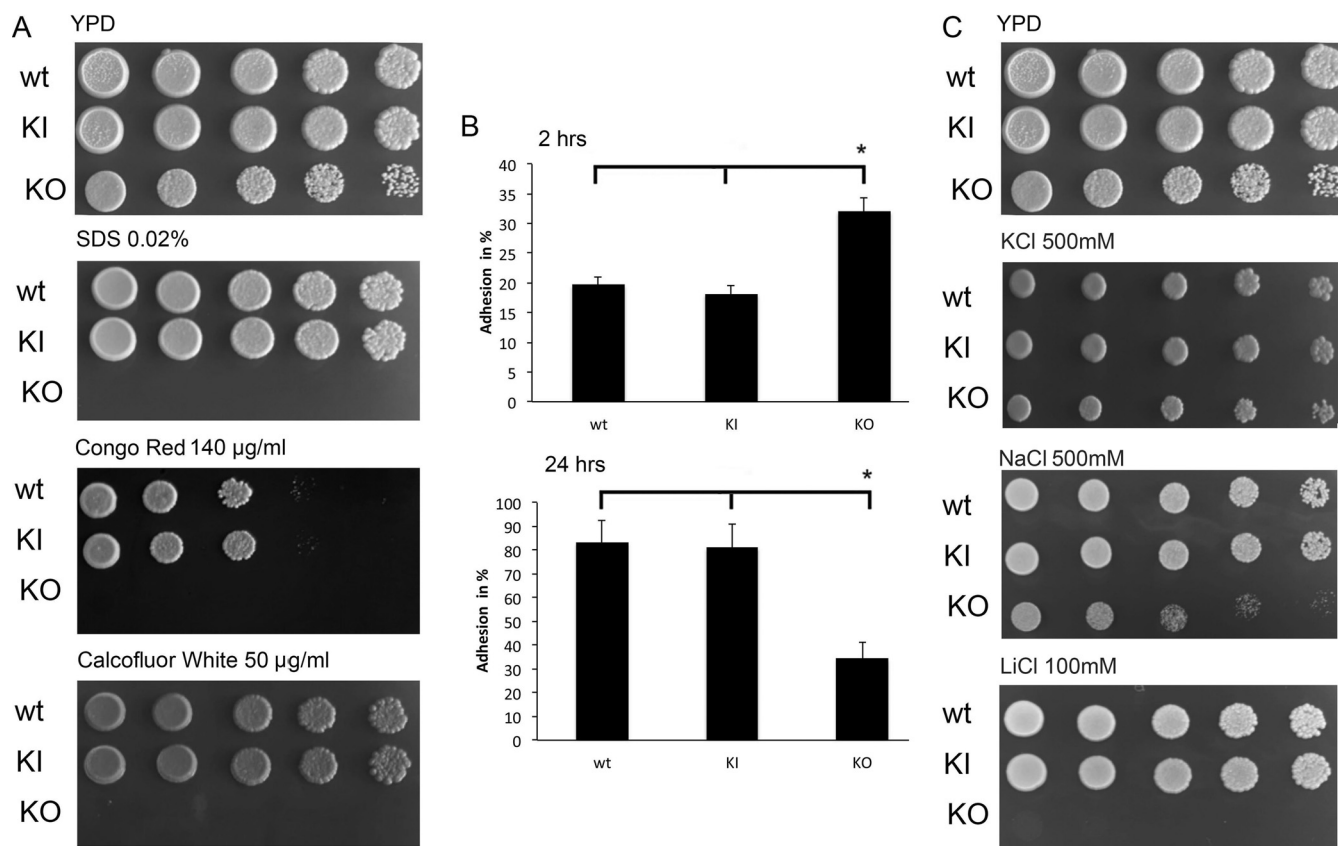


**FIG 4** The *ent2Δ/Δ* mutant strain has a decreased tolerance to cell wall stressors and salt stress. (A and C) The *ent2Δ/Δ* null mutant (KO), wild-type (wt), and knock-in (KI) strains were grown on YPD plates for 48 h containing cell wall stressors SDS (0.05%), calcofluor white (50  $\mu\text{g}/\text{ml}$ ), and Congo red (140  $\mu\text{g}/\text{ml}$ ) (A) as well as cationic cell stress conditions, including 500 mM KCl, 500 mM NaCl, or 100 mM LiCl (C). (B) The impact on adhesion to plastic surfaces (polystyrene) was measured using the XTT reduction assay in the *ent2Δ/Δ* null mutant (KO) and control strains (wt and KI) after 2 and 24 h of incubation on plastic surfaces. The images shown in panels A and C are representative of three different experiments. Error bars in panel B are the standard deviations of three different data sets. Each individual data point was run in triplicate and averaged. Statistical significance in panel B between control strains (wt and KI) and KO was determined with Student's *t* test (\*,  $P < 0.05$ ).

requires cellular internalization, since cytochrome P-450 is found either in the inner membrane of mitochondria or in the endoplasmic reticulum of cells. The other two antifungal agents, caspofungin and amphotericin B, function directly on the cell wall and plasma membrane by blocking the synthesis of  $\beta$  (1, 3)-D-glucan of the fungal cell wall or by binding to plasma membrane ergosterol and forming rapid leaking pores, respectively.

While the control YPD plate showed only a minor growth defect for the KO, when grown on YPD plates containing different concentrations of caspofungin and amphotericin B, the *C. albicans ent2Δ/Δ* (KO) exhibited a substantial growth defect at all concentrations of caspofungin (0.025 to 0.1  $\mu\text{g}/\text{ml}$ ) and at the highest concentration of amphotericin B (1.0  $\mu\text{g}/\text{ml}$ ) tested, respectively (Fig. 5A and B). Conversely, in the presence of fluconazole, the KO was less sensitive to the drug compared to the controls (Fig. 5C). While control strains exhibited a dramatic growth defect at 2 to 4  $\mu\text{g}/\text{ml}$ , growth of the KO strain was not affected. The results support the notion that a compromised cell wall and membrane will render the KO more vulnerable to caspofungin and amphotericin B. Since fluconazole has a different mode of action and requires cellular transport and processing, this finding is consistent with the conclusion that an intracellular trafficking defect in the *ent2Δ/Δ* mutant leads to greater resistance to fluconazole.

**C. albicans ENT2 impacts hyphal morphogenesis and biofilm formation.** To further investigate the implications of the impaired cell wall and intracellular transport defects, we focused on hyphal growth and the capacity for biofilm formation. Initially, we grew the *ent2Δ/Δ* strain (KO) at 37°C for 48 h on various plates with media that induced filamentation, such as M199 and RPMI 1640 media (Fig. 6A). While the wt and

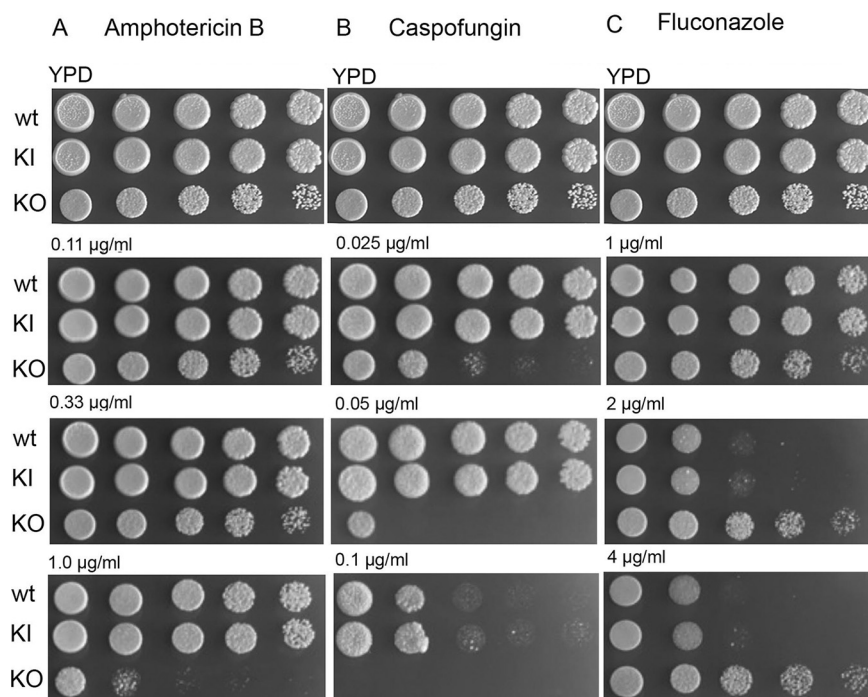


**FIG 5** The *ent2 $\Delta/\Delta$*  mutant strain has increased susceptibility to amphotericin B and caspofungin and reduced susceptibility to fluconazole. The *ent2 $\Delta/\Delta$*  null mutant (KO), wild-type (wt), and knock-in (KI) strains were grown on YPD plates for 48 h containing antifungal drugs at various concentrations as follows: amphotericin B at 0.11  $\mu\text{g/ml}$ , 0.33  $\mu\text{g/ml}$ , and 1.0  $\mu\text{g/ml}$  (A), caspofungin at 0.025  $\mu\text{g/ml}$ , 0.05  $\mu\text{g/ml}$ , and 0.1  $\mu\text{g/ml}$  (B), and fluconazole at 1.0  $\mu\text{g/ml}$ , 2.0  $\mu\text{g/ml}$ , and 4.0  $\mu\text{g/ml}$  (C). The images shown in panels A to C are representative of three different experiments.

KI control strains produced robust filaments indicated by an indistinct, filamentous rim around the cell colonies or in the center, the KO had a smooth rim and center under these conditions. To assess the morphological phenotype, we grew KO and control strains in RPMI 1640 medium at 37°C for 48 h and stained with calcofluor white. This stain revealed that the KO strain was growing as yeast, unlike the controls that formed hyphae under these strong inducing conditions (Fig. 6B).

To examine the role of *ENT2* in biofilm formation, we performed detailed studies of biofilm formation using the 2,3-bis-(2-methoxy-4-nitro-5-sulfonyl)-2H-tetrazolium-5-carboxanilide salt (XTT) reduction assay and differential interference contrast (DIC) light microscopy. The *ent2 $\Delta/\Delta$*  mutant (KO) forms a sparse, patchy, poorly adherent biofilm, which lifts easily with minimal disturbance, unlike the wt and KI strains (Fig. 6D). These observations are consistent with the KO strain's reduced adhesion capacity after 24 h (Fig. 3C). The biofilm's metabolic activity is reduced by 40% compared to the wt and KI strains (Fig. 6C). These results suggest that *ENT2* is required for normal filamentation and biofilm formation.

**Dissolution of cell-cell adhesions is impaired in the presence of the *C. albicans ent2 $\Delta/\Delta$*  strain.** Filamentation and the ability to form biofilms are key attributes of *C. albicans* virulence and a determinant of its pathogenesis. To assess the virulence of the *ent2 $\Delta/\Delta$*  strain (KO) compared to the controls, we tested the capability of this mutant to destroy cell-cell adhesion in human vaginal keratinocytes. The destruction of tight junctions between host cells is a hallmark of *C. albicans* virulence and is facilitated by digestion of the adhesion molecule E-cadherin by the proteases Sap4 to Sap6 (48, 49). We infected a vaginal human keratinocyte cell line VK-2 with the KO and the control strains (wt and KI) for 6 h and 24 h. We evaluated the cells over time for the presence of E-cadherin. Coculture with *C. albicans* KO, wt, or KI after 6 h of incubation revealed E-cadherin-labeled puncta at tight junctions between VK-2 cells. After 24 h, no staining was observed using the anti-E-cadherin antibody in VK-2 cells cocultured with wt and

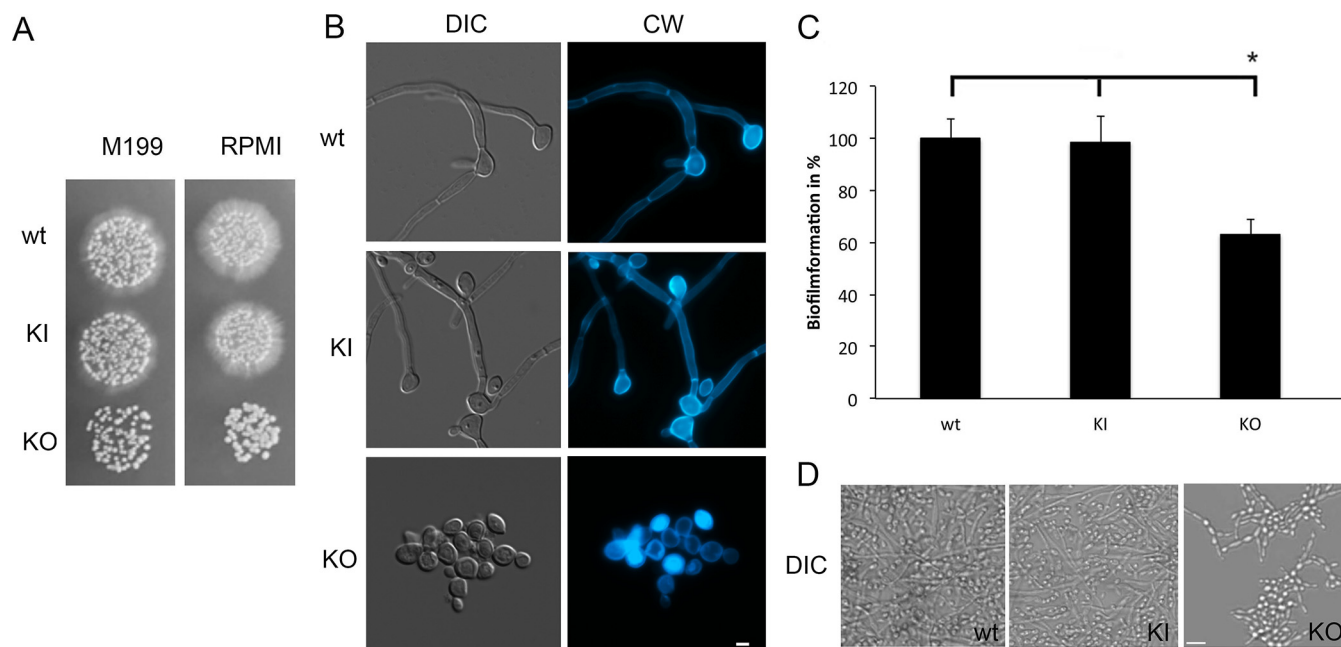


**FIG 6** The *ent2Δ/Δ* mutant does not form filaments and forms an aberrant biofilm. (A) The *ent2Δ/Δ* null mutant (KO), wild-type (wt), and knock-in (KI) strains were assayed on agar plates grown for 72 h at 37°C with different media (medium 199 [M199] and RPMI 1640 medium) known to induce hyphal growth. (B) These strains were grown on liquid RPMI 1640 medium overnight and were visualized by DIC and fluorescence microscopy after staining with calcofluor white (CW). The bar indicates 5  $\mu$ m. (C) Biofilms were grown on plastic surfaces with RPMI 1640 medium for 48 h and assayed for biofilm metabolic activity. (D) These biofilms were visualized by light microscopy using a DIC filter. The bar indicates 50  $\mu$ m. The images shown in panels A, B, and D are representative of three different experiments. Error bars in panel C are the standard deviations of three different data sets. Each individual data point was run in triplicate and averaged. Statistical significance in panel C between control strains (wt and KI) and KO was determined with Student's *t* test (\*,  $P < 0.05$ ).

KI (Fig. 7A). In contrast, in VK-2 cells exposed to KO strains, the E-cadherin-labeled tight junctions remained intact (Fig. 7A).

The presence of E-cadherin in VK-2 cells during coculture with *C. albicans* was analyzed by Western blotting (Fig. 7B). While at 6 h of incubation, E-cadherin levels were similar between cocultures, by 24 h, E-cadherin was undetectable in cells cocultured with wt and KI. In contrast, the E-cadherin level remained stable over time in VK-2 cells incubated with the KO strain (Fig. 7B). Consistent with this finding, in a bovine serum albumin (BSA) plate assay, we detected reduced protease activity in the KO compared to the controls (Fig. 7C).

Taken together, these findings suggest a reduction of protease activity in the *ent2Δ/Δ* mutant compared to control strains, resulting in reduced virulence as measured by the ability to disrupt cell-cell adhesion of vaginal keratinocytes.

**The *C. albicans ent2Δ/Δ* mutant lacks the ability to kill host cells.** To further define the virulence of the *ent2Δ/Δ* strain, we tested its ability to kill host cells. Using a microplate Live/Dead assay (Invitrogen, Waltham, MA), we evaluated human VK-2 cell growth after 6 h and 24 h of infection with the *ent2Δ/Δ* mutant and the KI and wt control strains. After 6 h of infection, 95% of VK-2 cells were alive in cultures with KO and the control strains (Fig. 8A). After 24 h, we found that while the KO was unable to kill VK-2 cells, the wt and KI strains killed 80% of host cells (Fig. 8B). This finding supports the notion of a substantially reduced virulence of the *ent2Δ/Δ* strain.

## DISCUSSION

In foundational studies, it was determined that secretory mutants display defects in endocytosis in the model *S. cerevisiae* (50). Recently, a clear linkage between clathrin-mediated endocytosis and the endosomal sorting complex required for transport (ESCRT)-dependent protein sorting pathway has been identified in *S. cerevisiae* (51). There it was found that members of the ESCRT complex are required for the viability of

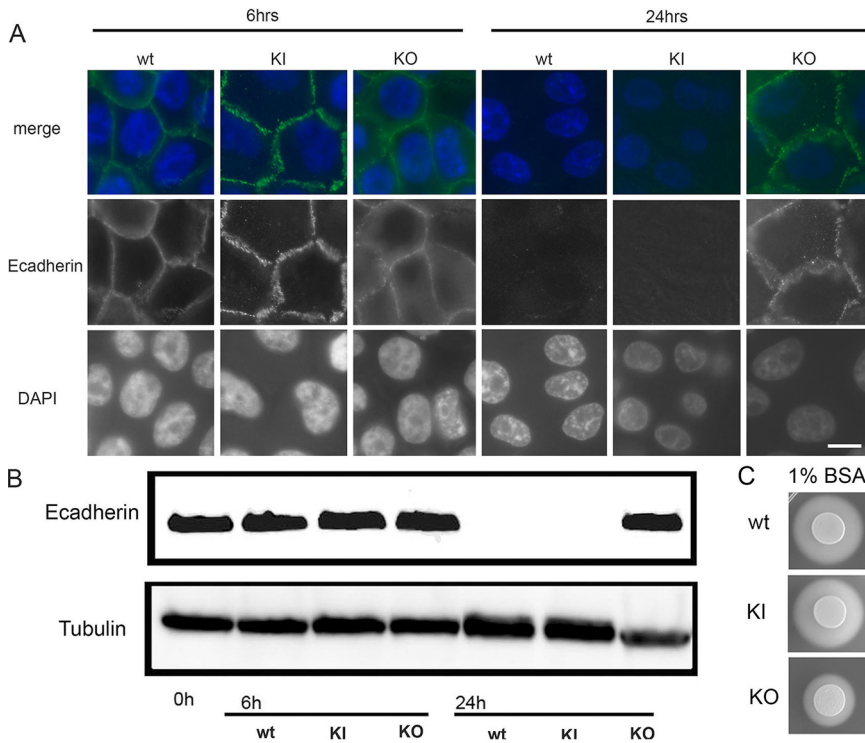


**FIG 7** The dissolution of cell-cell adhesions in human VK-2 cells is impaired in the presence of *C. albicans ent2Δ/Δ*. (A and B) Human VK-2 cells infected with the *ent2Δ/Δ* null mutant (KO), wild-type (wt), and knock-in (KI) strains for 6 and 24 h were visualized by fluorescence microscopy using an antibody against E-cadherin and DAPI for labeling the nucleus (A) and were tested by Western blotting for the proteins E-cadherin and tubulin (loading control) (B). (C) These *C. albicans* strains were further tested in a protease agar plate assay for their ability to lyse BSA after an overnight incubation at 30°C. The images shown in panel A to C are representative of three different experiments. The bar in panel A is 10 μm.

cells lacking the epsins Ent1p and Ent2p in which one ENTH domain has been reintroduced (51). In the prevacuolar secretory pathway, *S. cerevisiae VPS1* contributes to endocytosis as well (52). As we build upon our past studies of general and prevacuolar secretion in *C. albicans* (2, 5, 53, 54), followed more recently by studies of late secretion (55), we have now turned our attention to analyzing key components of endocytosis, as these pathways are interconnected and potentially share common elements.

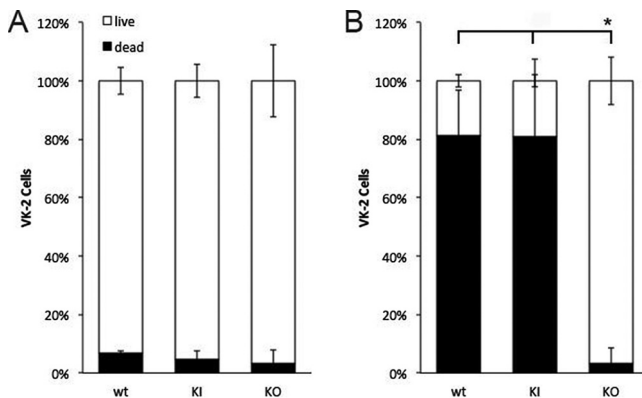


**FIG 8** The *C. albicans ent2Δ/Δ* mutant lacks the ability to kill human VK-2 cells. VK-2 cells infected with the *ent2Δ/Δ* null mutant (KO), wild-type (wt), and knock-in (KI) strains for 6 h (A) and 24 h (B) were tested in a Live/Dead assay. Error bars in panels A and B are the standard deviations of three different data sets. Each individual data point was run in triplicate and averaged. Statistical significance between control strains (wt and KI) and KO was determined with Student’s *t* test (\*, *P* < 0.05).

To our knowledge, epsins have not previously been investigated in *C. albicans*. Three putative genes, *ENT2*, *ENT3*, and *ENT4*, are annotated in the Candida Genome Database. In our alignment analysis, only *ENT2* demonstrated strong homology to *S. cerevisiae* *ENT1/2*, whereas the putative *C. albicans* genes *ENT3* and *ENT4* have only weak or no homology to the ENTH domain that is characteristic for binding the phosphorylated head group of the lipid PIP<sub>2</sub> in the nearby leaflet of a membrane bilayer, which disturbs the bilayer's stability and contributes to membrane bending (Fig. 1). Another characteristic domain for some epsins is the ubiquitin-interacting motif (UIM) which provides a binding site for cargo. Ent2p is the only known epsin in *C. albicans* with a UIM site (Fig. 1) suggesting that this protein has an important role in cargo selectivity during clathrin-mediated endocytosis.

Using a reverse genetic approach, our study sought to determine the contribution of the epsin Ent2p in endocytosis and the role of endocytic trafficking in *C. albicans* filamentation, biofilm formation, and virulence. While the *ent2Δ/Δ* mutant is viable, we detected a slight growth defect under regular growth conditions, suggesting nonessential functions that support optimal efficiency for endocytosis and intracellular transport (Fig. 2). This finding was in contrast to that of *S. cerevisiae*, where deletion of *ENT1* and *ENT2* was synthetically lethal (10, 56, 57). Since *ENT3* has much weaker homology to the ENTH domain and lacks other important endosomal protein domains such as the clathrin-binding domain and ubiquitin-interacting motifs (Fig. 1), These findings suggest that *ENT3* is unlikely to function as a redundant gene for *ENT2*.

Here, we have identified several roles for Ent2p in endocytosis, maintenance of cell wall/membrane integrity and protease function, and facilitating transport of antifungal drugs, dyes, and cations (Fig. 3, 4, 5, and 7). While in the *ent2Δ/Δ* mutant these transport processes are not completely stopped, the inefficiencies have downstream implications, such as the inability to form filaments and proper biofilms and greatly reduced virulence-related attributes (Fig. 6 and 8).

While we detected a defect in the endocytosis of FM4-64 (Fig. 3), we had several other findings that indicated other cellular transport processes were impaired as well. The cation sensitivity demonstrated with Na<sup>+</sup> and Li<sup>+</sup> (Fig. 4C) suggests that the transport of the cation pump is impaired. Indeed, the cation pump Ena1p in *S. cerevisiae* is recruited by Ent1/2p as cargo via an interaction with the UIM site (28, 57), although in *C. albicans* the cation pump has yet to be characterized.

We observed an impaired cell wall and an enhanced peripheral staining in the *ent2Δ/Δ* strain using cell wall/membrane dyes such as calcofluor white (CW) (Fig. 2D and E) and FM4-64 (see Fig. S5B in the supplemental material). Staining with CW, which binds to chitin, revealed an enhanced CW concentration in the KO strain compared to the control strains. One explanation could be increased chitin content of the cell wall of the KO, or possibly a looser packing of the chitin layer because of missing cell wall components that anchor the chitin to the cell wall. In contrast, FM4-64 is lipophilic and binds to the plasma membrane. Why we detected an increased level of CW and FM4-64 on the cell surface of the KO remains to be determined; further investigations are warranted to address this question. Changes in the cell wall integrity in the *ent2Δ/Δ* strain were revealed by several different cell wall stressors (Fig. 4A) and antifungal agents (casposfungin and amphotericin B; Fig. 5A and B) that impact the cell wall directly. An increased early adhesion capacity of the KO is potentially the result of changes in the cell wall integrity as well (Fig. 4B). All these findings support the possibility that transport and/or renewal of cell wall components is impaired.

Improperly functioning endocytic transport likely has implications on the secretion of extracellular components. Our data indicate that some or all aspartyl proteases are not secreted in the *ent2Δ/Δ* strain by demonstrating the inability of *ent2Δ/Δ* to break down E-cadherin in a vaginal epithelial cell line (Fig. 7A to C). Several studies have shown that the *C. albicans* proteases Sap4 to Sap6 are responsible for degrading E-cadherin in host cells (58). Taken together, these findings provide indirect evidence for impairments in

**TABLE 1** List of primers

Primer	Sequence	Reference
Hu EcadherintndF	GTC TGT AGG AAG GCA CAG CC	72
Hu EcadherintndR	TGC AAC GTC GTT ACG AGT CA	72
Hu GAPDHF	GGA CCT GAC CTG CCG TCT A	73
Hu GAPDHR	TGC TGT AGC CAA ATT CGT TG	73
ENT2 inner F	CCT CAA TCG CAA CAATTC CA	This study
ENT2 inner R	AGC GTT ACC AAA TCC ATA CCCA	This study
ENT2 outer F/donor KI	GCT GGT GGA GGA AAC TCA TAG CC	This study
ENT2 outer R/donor KI	GGG GAT ACC GAA ACC GTG T	This study
ENT2 probe Southern F	GGA ATT CGT GCG AAA CCG GA	This study
ENT2 probe Southern R	TAA AGT ATG GGC GGGCGT G	This study
ENT2 KO donor U.90	CCA AAT AAA AAG GGT TTA TAT CAT TAT ATA CGG ATT TTT GAA ATT AAT AGA TAT TTA AAC AAG TTC CAA TCA ACA ATA ATT GCT TTT TAG	This study
ENT2 KO donor L.90	CTA AAA AGC AAT TAT TGT TGA TTG GAA CTT GTT TAA ATA TCT ATT AAT TTC AAA AAT CCG TAA ATA ATG ATA TAA ACC CTT TTT ATT TGG	This study
ENT2 guide RNA oligo	CGT AAA CTA TTT TTA ATTTGC AAA CGT GGT GGG TCC AGT GGT TTT AGA GCTAGA AAT	This study
AHO1098	CAAATTAATAATAGTTTACGCAAG	62
AHO1099	GTT TTA GAG CTA GAA ATG CAA GTT	62

intracellular trafficking in the *ent2Δ/Δ* mutant. Future studies are under way to address this question.

In another body of experiments, we addressed the downstream effects of inefficient endocytic trafficking in the *ent2Δ/Δ* mutant. Since hyphal formation is crucially linked to dramatic changes of the cell wall and massive secretion of extracellular components, it was not surprising that the *ent2Δ/Δ* mutant is unable to form hyphae or to form a proper biofilm (Fig. 6A to D). This finding was associated with a greatly reduced virulence in our *in vitro* assays. The Live/Dead assay shows the inability of the *ent2Δ/Δ* mutant to kill host cells. The lack of hyphal growth and the limited ability to secrete proteases that degrade host cell E-cadherin provide a mechanistic explanation for this outcome.

This study represents the first characterization of the *C. albicans* epsin, Ent2p. We have identified that this epsin is involved in endocytosis and potentially other intracellular trafficking pathways. These processes become inefficient when Ent2p is missing, leading to an inability to form hyphae and loss of virulence-related attributes *in vitro*. Future work will address additional components of endocytosis, as we develop a detailed model of this process in *C. albicans*. The results of our study suggest that *C. albicans* Ent2p provides a link between endocytosis and other intracellular transport pathways, including exocytosis. It further suggests that unlike in *S. cerevisiae*, the role of Ent2p is not essential but supportive to ensure efficient intracellular trafficking.

## MATERIALS AND METHODS

**Identification of *C. albicans* ENT2.** The DNA and predicted protein sequences for *S. cerevisiae* ENT1 (YDL161W) and ENT2 (YLR206W) and for *C. albicans* ENT2 (C2\_01390W), ENT3 (C2\_02340C), and ENT4 (C3\_07280C) were retrieved from <http://www.yeastgenome.org> and <http://www.candidagenome.org>, respectively. A single potential ortholog to *S. cerevisiae* ENT1 was identified by a BLASTp search of the Candida Genome Database utilizing the functions on these websites. Alignments of multiple protein sequences were done by the SnapGene protein align function, MUSCLE (59). The degree of paired homologies was determined using the Smith-Waterman method (60) for local alignments. For clarity, large regions of low complexity and divergent sequence are omitted from Fig. 1. The areas of amino acid residues that were omitted are marked with parentheses. The web resource, Simple Modular Architecture Research Tool (SMART) (61), available at <https://smart.embl.de>, was utilized for the identification and annotation of protein domains.

**Deletion of *C. albicans* ENT2 and Southern blotting.** A list of oligonucleotides and primers used in this study is shown in Table 1. We generated a *C. albicans ent2Δ/Δ* null mutant using a CRISPR-Cas9 strategy developed by the Hernday laboratory (62). Alleles of ENT2 were then reintegrated via homologous recombination into the *ent2Δ* null mutant to generate a complemented “knock-in” (KI) strain. Correct strain construction was confirmed by Southern blotting of genomic DNA. Briefly, 5 μg genomic DNA was digested with BstXI overnight and loaded onto a 1% agarose gel. The blot was performed using a Hbond nylon membrane (Amersham/Sigma, St. Louis, MO) and a standard protocol. A DNA probe was generated by PCR using digoxigenin (DIG)-labeled deoxynucleoside triphosphate (dNTP)

**TABLE 2** List of strains

Strain	Description/genotype	Reference
AHY940	SC5314 <i>LEU2</i> heterozygous knockout $\alpha/leu2\Delta/LEU2$	62
CRENT2KO	SC5314 <i>ent2</i> homozygous knockout $\alpha/ent2\Delta/ent2\Delta$	This study
CRENT2KI	SC5314 <i>ENT2</i> homozygous knock-in $\alpha/ent2\Delta/ent2\Delta ENT2/ENT2$	This study

(Roche, Basel, Switzerland) and primers as shown in Table 1. Detection was performed using the DIG Luminescent Detection kit (Roche, Basel, Switzerland).

**Strains, media, and cell culture.** The *C. albicans* strains utilized in this study are listed in Table 2. YPD (1% yeast extract, 2% peptone, 2% glucose) or YNB (6.7 g yeast nitrogen base and 2% glucose) was used as a standard growth medium for overnight cultures (16 h). Percentages are weight/volume. Unless otherwise stated, liquid cell cultures were established by incubation at 30°C with shaking at 250 rpm.

VK-2/E6E7 cells (ATCC CRL-2616, Manassas, VA), a human vaginal keratinocyte cell line, were grown in keratinocyte SFM (serum free medium) (Invitrogen, Waltham, MA) in a cell culture incubator at 37°C with 5% CO<sub>2</sub>. Cells were split once a week and fed every 2 days.

**Preparation of plasmids and genomic DNA.** Competent *Escherichia coli* DH5 $\alpha$  cells (Invitrogen, Waltham, MA) were used to maintain plasmids. *E. coli* cells carrying plasmids of interest were grown in LB medium (1% tryptone, 0.5% glucose, and 1% NaCl) with 100  $\mu$ g/ml ampicillin at 37°C. Plasmid DNA was extracted from overnight cultures using the Qiagen Plasmid Miniprep system (Qiagen, Germantown, MD) according to the manufacturer's instructions. Plasmids used and generated in this study are listed in Table 3. Genomic DNA was extracted from yeast cells using the MasterPure Yeast DNA purification kit (Epicentre Biotechnologies, Madison, WI) according to the manufacturer's instructions.

**Western blotting for E-cadherin.** Western blotting was performed from lysed VK-2 cells infected with the *C. albicans ent2 $\Delta$ / $\Delta$*  mutant or control strains for 6 and 24 h in keratinocyte SFM medium at 37°C and 5% CO<sub>2</sub>. The standard protocol is described in reference 63. Primary antibodies to E-cadherin (R&D Systems, Minneapolis, MN) and tubulin (Invitrogen, Waltham, MA) were incubated overnight and were used at 1:500 and 1:1,000 dilutions, respectively. Anti-mouse secondary antibody (Invitrogen, Waltham, MA) was incubated for 1 h in a 1:10,000 dilution. Tubulin was used as a loading control.

**Cell growth assay and agar plate assays for response to cell wall stressors, salt stress, and filamentation.** From an overnight culture in YPD at 30°C, cells were counted and diluted in YPD to a cell concentration of  $1 \times 10^6$  cells/ml. One hundred microliters of this cell dilution was placed in 96-well plates in quadruplicate. Cell growth was determined over 15 h at 30°C using a microplate reader (BioTek Synergy H1; BioTek, Winooski, VT) that recorded the extinction at an optical density at 600 nm (OD<sub>600</sub>) every 30 min.

Growth rates were assessed on agar plate assays after 48 h as described previously (64, 65). Growth was assayed in response to 30°C and 37°C, cell wall stressors (0.2% SDS in YPD, 140  $\mu$ g/ml Congo red in YNB with 2% glucose (YNB/glucose), 50  $\mu$ g/ml calcofluor white in YNB/glucose [all from Sigma-Aldrich, St. Louis, MO]), potassium chloride, lithium chloride, and sodium chloride (all Sigma-Aldrich, St. Louis, MO) in YPD, BSA with YNB/glucose (66) as well as antifungal drugs (amphotericin B, caspofungin, fluconazole [all Sigma-Aldrich, St. Louis, MO] in YPD). Filamentation was determined after 48 h at 37°C on medium 199 supplemented with L-glutamine (M199; Sigma-Aldrich, St. Louis, MO), and RPMI 1640 medium (pH 7.0) (Fisher Scientific, Waltham, MA) (67). Five-microliter portions of cells from 1:5 serial dilutions were spotted onto agar plates.

**Analyses of endocytosis.** The lipophilic membrane dye FM4-64 [*N*-(3-triethylammoniumpropyl)-4-(6-(4-(diethylamino)phenyl)hexatrienyl) pyridiniumdibromide] (EMD Millipore, Temecula, CA), which is actively endocytosed, was used to assay membrane-related endocytosis as described previously (39). Briefly, *C. albicans* strains were grown in YPD at 30°C to mid-log phase. An aliquot of cells was resuspended in fresh, ice-cold YPD. FM4-64 at a final concentration of 2 mM was added and incubated on ice for 20 min. The cells were washed five times in ice-cold phosphate-buffered saline (PBS) and then resuspended in fresh YPD at room temperature. Next, the cells were incubated at room temperature and harvested at 5, 15, and 30 min. Membrane transport at each time point was stopped with ice-cold 12 mM sodium azide (Sigma-Aldrich, St. Louis, MO). Staining of the vacuoles was visualized using a Zeiss ImagerM1 fluorescence microscope. Images were taken using standard Texas Red filters for FM4-64. For the statistical analysis, we have analyzed the stain of the vacuolar membrane in 100 cells per strain and condition. The average of three experiments was determined and expressed as a percentage of the total number of cells counted.

**Analysis of adherence and biofilm formation in *C. albicans* endocytosis mutants.** Biofilms were visualized via DIC light microscopy on a Nikon Eclipse Ti inverted microscope, and metabolic activity was measured by XTT reduction, in triplicate, according to published methods (68).

**TABLE 3** List of plasmids

Plasmid	Description	Reference
pADH137	<i>C. albicans</i> LEUpOUT CAS9 expression plasmid	62
pADH118	<i>C. albicans</i> LEUpOUT "blank" gRNA plasmid	62
pCRENT2	<i>C. albicans</i> LEUpOUT "blank" gRNA plasmid with <i>ENT2</i> guide RNA	This study

Adhesion to polystyrene was assessed as described previously (69) with minor modifications. Briefly, an inoculum of  $1.0 \times 10^7$  cells  $\text{ml}^{-1}$  in PBS or RPMI 1640 medium was prepared. One hundred fifty microliters of cell suspension was added to individual wells of a 96-well microtiter plate. An identical set of each strain was dispensed into individual microcentrifuge tubes for use as the unwashed control, representing the total number of adherent and nonadherent cells. Following 2 and 24 h of incubation at 37°C, nonadherent cells were removed by washing the wells of the 96-well plate, while cells incubated in microcentrifuge tubes were pelleted at 5,000 rpm in a benchtop centrifuge. The XTT reduction assay was then used to quantify the adhered and total amount of cells in each well and microcentrifuge tube, respectively. After incubation with the XTT-menadione substrate at 37°C for 3 h, 75  $\mu\text{l}$  of supernatant was transferred to a fresh 96-well plate, and absorbance was read at 490 nm in a microplate reader (BioTek Synergy H1; BioTek, Winooski, VT). The adherence capacity of each strain was calculated as the mean XTT value of the washed cells relative to the mean XTT value of the unwashed cells. Experiments were performed in triplicates, each with eight replicates per strain. Statistical significance was assessed using a Student *t* test in Microsoft Excel.

**Immunofluorescence microscopy and quantitative plate assay of *C. albicans* strains with CW staining.** Cell morphology of yeast and hyphal forms was assessed via fluorescence microscopy as described previously (70). Cells from an overnight culture in YPD at 30°C (yeast growth) or 37°C in RPMI 1640 medium (filamentous growth) were mixed 20:1 with calcofluor white (Sigma-Aldrich, St. Louis, MO), placed on a slide and visualized with a 63 $\times$  lens and 4',6-diamidino-2-phenylindole (DAPI) filter of a Nikon Eclipse 80i microscope. For the quantitative plate assay,  $10^6$  cells from each strain were mixed 20:1 with calcofluor white and incubated for 30 min. Cells were washed six times with ice-cold PBS, resuspended in 300  $\mu\text{l}$ , and placed in triplicate wells of 100- $\mu\text{l}$  solutions into 96-well plates. The plate was read in a microplate reader (BioTek Synergy H1; BioTek, Winooski, VT) using excitation and emission filters for CW (380 nm and 475 nm, respectively). The resulting data were analyzed according to the manufacturer's instruction using Excel (Microsoft).

**Immunofluorescence microscopy of cocultured VK-2 cells with *C. albicans* strains.** VK-2 cells growing on coverslips were infected with *C. albicans ent2 $\Delta$ / $\Delta$*  or control strains for 6 and 24 h in keratinocyte SFM medium at 37°C and 5%  $\text{CO}_2$ , as described previously (71). Cocultured *C. albicans* and VK-2 cells were fixed with 4% paraformaldehyde solution and incubated for 20 min. Next, the coverslips were washed with 1 $\times$  PBS. The fixed cells were incubated with ammonium chloride for 10 min, followed by incubation with Triton X-100 for 5 min. Cells were then washed three times with PBS containing 0.2% gelatin at 5 min each. VK-2 cells were stained for 1 h with a 1:100 dilution of a E-cadherin primary antibody (R&D, Minneapolis, MN) in PBS containing 0.2% gelatin, washed, and incubated with an anti-mouse-green fluorescent protein (GFP) secondary antibody (Invitrogen, Waltham, MA) for another hour. Cover slides were mounted on slides with an antifade mounting solution containing DAPI. A Nikon Eclipse 80i microscope was used to visualize the cells using standard GFP and DAPI filters.

**Live/Dead viability assay.** VK-2 cells were grown in 96-well plates in a serum-free medium (SFM) to 30% confluence. *C. albicans* strains were grown overnight in YPD and were cocultured with VK-2 cells at a concentration of  $5 \times 10^5$  cell/ml for 6 and 24 h. The Live/Dead viability assay from Invitrogen (Waltham, MA) was performed using the protocol provided by the manufacturer. In brief, controls were uninfected cells and killed cells using 70% methanol for 30 min. Ethidium bromide (8  $\mu\text{M}$ ) and calcein-AM (4  $\mu\text{M}$ ) were mixed, and 100  $\mu\text{l}$  was added to each well, and plates were incubated for 30 min. The plate was read in a microplate reader (BioTek Synergy H1; BioTek, Winooski, VT) using excitation and emission filters for ethidium bromide (495 nm and 635 nm, respectively) and calcein-AM (495 nm and 515 nm, respectively). The resulting data were analyzed according to the manufacturer's instruction using Excel (Microsoft).

## SUPPLEMENTAL MATERIAL

Supplemental material is available online only.

**FIG S1**, TIF file, 0.1 MB.

**FIG S2**, TIF file, 0.8 MB.

**FIG S3**, TIF file, 0.04 MB.

**FIG S4**, TIF file, 0.04 MB.

**FIG S5**, TIF file, 0.4 MB.

## REFERENCES

- Lee SA, Jones J, Khaliq Z, Kot J, Alba M, Bernardo S, Seghal A, Wong B. 2007. A functional analysis of the *Candida albicans* homolog of *Saccharomyces cerevisiae* VPS4. *FEMS Yeast Res* 7:973–985. <https://doi.org/10.1111/j.1567-1364.2007.00253.x>.
- Lee SA, Jones J, Hardison S, Kot J, Khaliq Z, Bernardo SM, Lazzell A, Monteagudo C, Lopez-Ribot J. 2009. *Candida albicans* VPS4 is required for secretion of aspartyl proteases and in vivo virulence. *Mycopathologia* 167:55–63. <https://doi.org/10.1007/s11046-008-9155-7>.
- Rane HS, Hardison S, Botelho C, Bernardo SM, Wormley F, Lee SA. 2014. *Candida albicans* VPS4 contributes differentially to epithelial and mucosal pathogenesis. *Virulence* 5:810–818. <https://doi.org/10.4161/21505594.2014.956648>.
- Martin R, Hellwig D, Schaub Y, Bauer J, Walther A, Wendland J. 2007. Functional analysis of *Candida albicans* genes whose *Saccharomyces cerevisiae* homologues are involved in endocytosis. *Yeast* 24:511–522. <https://doi.org/10.1002/yea.1489>.
- Palanisamy SKA, Ramirez MA, Lorenz M, Lee SA. 2010. *Candida albicans* PEP12 is required for biofilm integrity and in vivo virulence. *Eukaryot Cell* 9:266–277. <https://doi.org/10.1128/EC.00295-09>.
- Feyder S, De Craene J-O, Bär S, Bertazzi DL, Friant S. 2015. Membrane trafficking in the yeast *Saccharomyces cerevisiae* model. *Int J Mol Sci* 16:1509–1525. <https://doi.org/10.3390/ijms16011509>.
- Goode BL, Eskin JA, Wendland B. 2015. Actin and endocytosis in budding yeast. *Genetics* 199:315–358. <https://doi.org/10.1534/genetics.112.145540>.

8. Carroll SY, Stimpson HEM, Weinberg J, Toret CP, Sun Y, Drubin DG. 2012. Analysis of yeast endocytic site formation and maturation through a regulatory transition point. *Mol Biol Cell* 23:657–668. <https://doi.org/10.1091/mbc.E11-02-0108>.
9. Stimpson HEM, Toret CP, Cheng AT, Pauly BS, Drubin DG. 2009. Early-arriving Syt1p and Ede1p function in endocytic site placement and formation in budding yeast. *Mol Biol Cell* 20:4640–4651. <https://doi.org/10.1091/mbc.e09-05-0429>.
10. Wendland B, Steece KE, Emr SD. 1999. Yeast epsins contain an essential N-terminal ENTH domain, bind clathrin and are required for endocytosis. *EMBO J* 18:4383–4393. <https://doi.org/10.1093/emboj/18.16.4383>.
11. Wendland B, Emr SD. 1998. Pan1p, yeast eps15, functions as a multivalent adaptor that coordinates protein-protein interactions essential for endocytosis. *J Cell Biol* 141:71–84. <https://doi.org/10.1083/jcb.141.1.71>.
12. Sun Y, Leong NT, Wong T, Drubin DG. 2015. A Pan1/End3/Sla1 complex links Arp2/3-mediated actin assembly to sites of clathrin-mediated endocytosis. *Mol Biol Cell* 26:3841–3856. <https://doi.org/10.1091/mbc.E15-04-0252>.
13. Feliciano D, Di Pietro SM. 2012. SLAC, a complex between Sla1 and Las17, regulates actin polymerization during clathrin-mediated endocytosis. *Mol Biol Cell* 23:4256–4272. <https://doi.org/10.1091/mbc.E11-12-1022>.
14. Bénédicti H, Raths S, Crausaz F, Riezman H. 1994. The END3 gene encodes a protein that is required for the internalization step of endocytosis and for actin cytoskeleton organization in yeast. *Mol Biol Cell* 5:1023–1037. <https://doi.org/10.1091/mbc.5.9.1023>.
15. Whitworth K, Bradford MK, Camara N, Wendland B. 2014. Targeted disruption of an EH-domain protein endocytic complex, Pan1-End3: Pan1 central region binds C-terminal End3 repeats. *Traffic* 15:43–59. <https://doi.org/10.1111/tra.12125>.
16. Tang HY, Cai M. 1996. The EH-domain-containing protein Pan1 is required for normal organization of the actin cytoskeleton in *Saccharomyces cerevisiae*. *Mol Cell Biol* 16:4897–4914. <https://doi.org/10.1128/MCB.16.9.4897>.
17. Sun Y, Leong NT, Jiang T, Tangara A, Darzacq X, Drubin DG. 2017. Switch-like Arp2/3 activation upon WASP and WIP recruitment to an apparent threshold level by multivalent linker proteins in vivo. *Elife* 6:e29140. <https://doi.org/10.7554/eLife.29140>.
18. Sen A, Madhivanan K, Mukherjee D, Aguilar RC. 2012. The epsin protein family: coordinators of endocytosis and signaling. *Biomol Concepts* 3:117–126. <https://doi.org/10.1515/bmc-2011-0060>.
19. Brett TJ, Traub LM, Fremont DH. 2002. Accessory protein recruitment motifs in clathrin-mediated endocytosis. *Structure* 10:797–809. [https://doi.org/10.1016/s0969-2126\(02\)00784-0](https://doi.org/10.1016/s0969-2126(02)00784-0).
20. Watson HA, Cope MJ, Groen AC, Drubin DG, Wendland B. 2001. In vivo role for actin-regulating kinases in endocytosis and yeast epsin phosphorylation. *Mol Biol Cell* 12:3668–3679. <https://doi.org/10.1091/mbc.12.11.3668>.
21. Newpher TM, Smith RP, Lemmon V, Lemmon SK. 2005. In vivo dynamics of clathrin and its adaptor-dependent recruitment to the actin-based endocytic machinery in yeast. *Dev Cell* 9:87–98. <https://doi.org/10.1016/j.devcel.2005.04.014>.
22. Aguilar RC, Longhi SA, Shaw JD, Yeh L-Y, Kim S, Schön A, Freire E, Hsu A, McCormick WK, Watson HA, Wendland B. 2006. Epsin N-terminal homology domains perform an essential function regulating Cdc42 through binding Cdc42 GTPase-activating proteins. *Proc Natl Acad Sci U S A* 103:4116–4121. <https://doi.org/10.1073/pnas.0510513103>.
23. Ford MGJ, Mills IG, Peter BJ, Vallis Y, Praefcke GJK, Evans PR, McMahon HT. 2002. Curvature of clathrin-coated pits driven by epsin. *Nature* 419:361–366. <https://doi.org/10.1038/nature01020>.
24. Yamamoto W, Wada S, Nagano M, Aoshima K, Siekhaus DE, Toshima JY, Toshima J. 2018. Distinct roles for plasma membrane PtdIns(4)P and PtdIns(4,5)P<sub>2</sub> during receptor-mediated endocytosis in yeast. *J Cell Sci* 131:jcs207696. <https://doi.org/10.1242/jcs.207696>.
25. Steinem C, Meinecke M. 2021. ENTH domain-dependent membrane remodeling. *Soft Matter* 17:233–240. <https://doi.org/10.1039/c9sm02437a>.
26. Legendre-Guillemain V, Wasiaik S, Hussain NK, Angers A, McPherson P. 2004. ENTH/ANTH proteins and clathrin-mediated membrane budding. *J Cell Sci* 117:9–18. <https://doi.org/10.1242/jcs.00928>.
27. Dores MR, Schnell JD, Maldonado-Baez L, Wendland B, Hicke L. 2010. The function of yeast epsin and Ede1 ubiquitin-binding domains during receptor internalization. *Traffic* 11:151–160. <https://doi.org/10.1111/j.1600-0854.2009.01003.x>.
28. Sen A, Hsieh W-C, Hanna CB, Hsu C-C, Pearson M, Tao WA, Aguilar RC. 2020. The Na<sup>+</sup> pump Ena1 is a yeast epsin-specific cargo requiring its ubiquitination and phosphorylation sites for internalization. *J Cell Sci* 133:jcs245415. <https://doi.org/10.1242/jcs.245415>.
29. Bar-Yosef H, Vivanco Gonzalez N, Ben-Aroya S, Kron SJ, Kornitzer D. 2017. Chemical inhibitors of *Candida albicans* hyphal morphogenesis target endocytosis. *Sci Rep* 7:5692. <https://doi.org/10.1038/s41598-017-05741-y>.
30. Bar-Yosef H, Gildor T, Ramirez-Zavala B, Schmauch C, Weissman Z, Pinsky M, Naddaf R, Morschhäuser J, Arkowitz RA, Kornitzer D. 2018. A global analysis of kinase function in *Candida albicans* hyphal morphogenesis reveals a role for the endocytosis regulator Akl1. *Front Cell Infect Microbiol* 8:17. <https://doi.org/10.3389/fcimb.2018.00017>.
31. Kay BK, Yamabhai M, Wendland B, Emr SD. 1999. Identification of a novel domain shared by putative components of the endocytic and cytoskeletal machinery. *Protein Sci* 8:435–438. <https://doi.org/10.1110/ps.8.2.435>.
32. Polo S, Sigismund S, Faretta M, Guidi M, Capua MR, Bossi G, Chen H, De Camilli P, Di Fiore PP. 2002. A single motif responsible for ubiquitin recognition and monoubiquitination in endocytic proteins. *Nature* 416:451–455. <https://doi.org/10.1038/416451a>.
33. Shih SC, Katzmann DJ, Schnell JD, Sutanto M, Emr SD, Hicke L. 2002. Epsins and Vps27p/Hrs contain ubiquitin-binding domains that function in receptor endocytosis. *Nat Cell Biol* 4:389–393. <https://doi.org/10.1038/ncb790>.
34. Oldham CE, Mohny RP, Miller SLH, Hanes RN, O'Bryan JP. 2002. The ubiquitin-interacting motifs target the endocytic adaptor protein epsin for ubiquitination. *Curr Biol* 12:1112–1116. [https://doi.org/10.1016/S0960-9822\(02\)00900-4](https://doi.org/10.1016/S0960-9822(02)00900-4).
35. Di Fiore PP, Polo S, Hofmann K. 2003. When ubiquitin meets ubiquitin receptors: a signalling connection. *Nat Rev Mol Cell Biol* 4:491–497. <https://doi.org/10.1038/nrm1124>.
36. Polo S, Confalonieri S, Salcini AE, Di Fiore PP. 2003. EH and UIM: endocytosis and more. *Sci STKE* 2003:re17. <https://doi.org/10.1126/stke.2132003re17>.
37. Sen A, Hsieh WH, Claudio R. 2017. The information content of glutamine-rich sequences define protein functional characteristics. *Proc IEEE Inst Electr Electron Eng* 105:385–393. <https://doi.org/10.1109/JPROC.2016.2613076>.
38. Dell'Angelica EC. 2001. Clathrin-binding proteins: got a motif? Join the network! *Trends Cell Biol* 11:315–318. [https://doi.org/10.1016/s0962-8924\(01\)02043-8](https://doi.org/10.1016/s0962-8924(01)02043-8).
39. Lettner A, Zeidler U, Gimona M, Hauser M, Breitenbach M, Bito A. 2010. *Candida albicans* AGE3, the ortholog of the *S. cerevisiae* ARF-GAP-encoding gene GCS1, is required for hyphal growth and drug resistance. *PLoS One* 5:e11993. <https://doi.org/10.1371/journal.pone.0011993>.
40. Ke R, Ingram PJ, Haynes K. 2013. An integrative model of ion regulation in yeast. *PLoS Comput Biol* 9:e1002879. <https://doi.org/10.1371/journal.pcbi.1002879>.
41. Prior C, Potier S, Souciet JL, Sychrova H. 1996. Characterization of the NHA1 gene encoding a Na<sup>+</sup>/H<sup>+</sup>-antiporter of the yeast *Saccharomyces cerevisiae*. *FEBS Lett* 387:89–93. [https://doi.org/10.1016/0014-5793\(96\)00470-x](https://doi.org/10.1016/0014-5793(96)00470-x).
42. Bañuelos MA, Quintero FJ, Rodríguez-Navarro A. 1995. Functional expression of the ENA1(PMR2)-ATPase of *Saccharomyces cerevisiae* in *Schizosaccharomyces pombe*. *Biochim Biophys Acta* 1229:233–238. [https://doi.org/10.1016/0005-2728\(95\)00006-5](https://doi.org/10.1016/0005-2728(95)00006-5).
43. Bañuelos MA, Sychrová H, Bleykasten-Grosshans C, Souciet J-L, Potier S. 1998. The Nha1 antiporter of *Saccharomyces cerevisiae* mediates sodium and potassium efflux. *Microbiology (Reading)* 144:2749–2758. <https://doi.org/10.1099/00221287-144-10-2749>.
44. Ferrando A, Kron SJ, Rios G, Fink GR, Serrano R. 1995. Regulation of cation transport in *Saccharomyces cerevisiae* by the salt tolerance gene HAL3. *Mol Cell Biol* 15:5470–5481. <https://doi.org/10.1128/MCB.15.10.5470>.
45. Ganster RW, McCartney RR, Schmidt MC. 1998. Identification of a calcineurin-independent pathway required for sodium ion stress response in *Saccharomyces cerevisiae*. *Genetics* 150:31–42. <https://doi.org/10.1093/genetics/150.1.31>.
46. Mendoza I, Rubio F, Rodríguez-Navarro A, Pardo JM. 1994. The protein phosphatase calcineurin is essential for NaCl tolerance of *Saccharomyces cerevisiae*. *J Biol Chem* 269:8792–8796. [https://doi.org/10.1016/S0021-9258\(17\)37038-2](https://doi.org/10.1016/S0021-9258(17)37038-2).
47. Märquez J, Serrano R. 1996. Multiple transduction pathways regulate the sodium-extrusion gene PMR2/ENA1 during salt stress in yeast. *FEBS Lett* 382:89–92. [https://doi.org/10.1016/0014-5793\(96\)00157-3](https://doi.org/10.1016/0014-5793(96)00157-3).
48. Vasioukhin V, Bauer C, Yin M, Fuchs E. 2000. Directed actin polymerization is the driving force for epithelial cell-cell adhesion. *Cell* 100:209–219. [https://doi.org/10.1016/s0092-8674\(00\)81559-7](https://doi.org/10.1016/s0092-8674(00)81559-7).
49. Gumbiner BM. 2005. Regulation of cadherin-mediated adhesion in morphogenesis. *Nat Rev Mol Cell Biol* 6:622–634. <https://doi.org/10.1038/nrm1699>.

50. Riezman H. 1985. Endocytosis in yeast: several of the yeast secretory mutants are defective in endocytosis. *Cell* 40:1001–1009. [https://doi.org/10.1016/0092-8674\(85\)90360-5](https://doi.org/10.1016/0092-8674(85)90360-5).
51. Hoban K, Lux SY, Poprawski J, Zhang Y, Shepherdson J, Castiñeira PG, Pesari S, Yao T, Prosser DC, Norris C, Wendland B. 2020. ESCRT-dependent protein sorting is required for the viability of yeast clathrin-mediated endocytosis mutants. *Traffic* 21:430–450. <https://doi.org/10.1111/tra.12731>.
52. Smaczynska-de Rooij II, Allwood EG, Aghamohammadzadeh S, Hettema EH, Goldberg MW, Ayscough KR. 2010. A role for the dynamin-like protein Vps1 during endocytosis in yeast. *J Cell Sci* 123:3496–3506. <https://doi.org/10.1242/jcs.070508>.
53. Lee SA, Mao Y, Zhang Z, Wong B. 2001. Overexpression of a dominant-negative allele of YPT1 inhibits growth and aspartyl protease secretion in *Candida albicans*. *Microbiology (Reading)* 147:1961–1970. <https://doi.org/10.1099/00221287-147-7-1961>.
54. Bernardo SM, Khalique Z, Kot J, Jones JK, Lee SA. 2008. *Candida albicans* VPS1 contributes to protease secretion, filamentation, and biofilm formation. *Fungal Genet Biol* 45:861–877. <https://doi.org/10.1016/j.fgb.2008.01.001>.
55. Bernardo SM, Rane HS, Chavez-Dozal A, Lee SA. 2014. Secretion and filamentation are mediated by the *Candida albicans* t-SNAREs Sso2p and Sec9p. *FEMS Yeast Res* 14:762–775. <https://doi.org/10.1111/1567-1364.12165>.
56. Zheng B, Wu JN, Schober W, Lewis DE, Vida T. 1998. Isolation of yeast mutants defective for localization of vacuolar vital dyes. *Proc Natl Acad Sci U S A* 95:11721–11726. <https://doi.org/10.1073/pnas.95.20.11721>.
57. Aguilar RC, Watson HA, Wendland B. 2003. The yeast epsin Ent1 is recruited to membranes through multiple independent interactions. *J Biol Chem* 278:10737–10743. <https://doi.org/10.1074/jbc.M211622200>.
58. Villar CC, Kashleva H, Nobile CJ, Mitchell AP, Dongari-Bagtzoglou A. 2007. Mucosal tissue invasion by *Candida albicans* is associated with E-cadherin degradation, mediated by transcription factor Rim101p and protease Sap5p. *Infect Immun* 75:2126–2135. <https://doi.org/10.1128/IAI.00054-07>.
59. Edgar RC. 2004. MUSCLE: multiple sequence alignment with high accuracy and high throughput. *Nucleic Acids Res* 32:1792–1797. <https://doi.org/10.1093/nar/gkh340>.
60. Smith TF, Waterman MS. 1981. Identification of common molecular subsequences. *J Mol Biol* 147:195–197. [https://doi.org/10.1016/0022-2836\(81\)90087-5](https://doi.org/10.1016/0022-2836(81)90087-5).
61. Schultz J, Milpetz F, Bork P, Ponting CP. 1998. SMART, a simple modular architecture research tool: identification of signaling domains. *Proc Natl Acad Sci U S A* 95:5857–5864. <https://doi.org/10.1073/pnas.95.11.5857>.
62. Nguyen N, Quail MMF, Hernday AD. 2017. An efficient, rapid, and recyclable system for CRISPR-mediated genome editing in *Candida albicans*. *mSphere* 2:e00149-17. <https://doi.org/10.1128/mSphereDirect.00149-17>.
63. Kurien BT, Scofield RH. 2006. Western blotting. *Methods* 38:283–293. <https://doi.org/10.1016/j.ymeth.2005.11.007>.
64. Bernardo SM, Lee SA. 2010. *Candida albicans* SUR7 contributes to secretion, biofilm formation, and macrophage killing. *BMC Microbiol* 10:133. <https://doi.org/10.1186/1471-2180-10-133>.
65. Rane HS, Bernardo SM, Raines SM, Binder JL, Parra KJ, Lee SA. 2013. *Candida albicans* VMA3 is necessary for V-ATPase assembly and function and contributes to secretion and filamentation. *Eukaryot Cell* 12:1369–1382. <https://doi.org/10.1128/EC.00118-13>.
66. Crandall M, Edwards JE. 1987. Segregation of proteinase-negative mutants from heterozygous *Candida albicans*. *J Gen Microbiol* 133:2817–2824. <https://doi.org/10.1099/00221287-133-10-2817>.
67. Liu H, Köhler J, Fink GR. 1994. Suppression of hyphal formation in *Candida albicans* by mutation of a STE12 homolog. *Science* 266:1723–1726. <https://doi.org/10.1126/science.7992058>.
68. Ramage G, López-Ribot JL. 2005. Techniques for antifungal susceptibility testing of *Candida albicans* biofilms. *Methods Mol Med* 118:71–79. <https://doi.org/10.1385/1-59259-943-5-071>.
69. Imbert C, Rodier MH, Daniault G, Jacquemin JL. 2002. Influence of sub-inhibitory concentrations of conventional antifungals on metabolism of *Candida albicans* and on its adherence to polystyrene and extracellular matrix proteins. *Med Mycol* 40:123–129. <https://doi.org/10.1080/mmy.40.2.123.129>.
70. Pringle JR, Adams AE, Drubin DG, Haarer BK. 1991. Immunofluorescence methods for yeast. *Methods Enzymol* 194:565–602. [https://doi.org/10.1016/0076-6879\(91\)94043-c](https://doi.org/10.1016/0076-6879(91)94043-c).
71. Rollenhagen C, Wöllert T, Langford GM, Sundstrom P. 2009. Stimulation of cell motility and expression of late markers of differentiation in human oral keratinocytes by *Candida albicans*. *Cell Microbiol* 11:946–966. <https://doi.org/10.1111/j.1462-5822.2009.01303.x>.
72. Farmakovskaya M, Khromova N, Rybko V, Dugina V, Kopnin B, Kopnin P. 2016. E-cadherin repression increases amount of cancer stem cells in human A549 lung adenocarcinoma and stimulates tumor growth. *Cell Cycle* 15:1084–1092. <https://doi.org/10.1080/15384101.2016.1156268>.
73. Rollenhagen C, Asin SN. 2010. IL-8 decreases HIV-1 transcription in peripheral blood lymphocytes and ectocervical tissue explants. *J Acquir Immune Defic Syndr* 54:463–469. <https://doi.org/10.1097/QAI.0b013e3181e5e12c>.